Remnants of the early Solar System water enriched in heavy oxygen isotopes

Naoya Sakamoto[1], Yusuke Seto[1], Shoichi Itoh[1], Kiyoshi Kuramoto[2], Kiyoshi Fujino[1], Kazuhide Nagashima[3], Alexander N. Krot[3] and Hisayoshi Yurimoto[1, 4]*

[1] Department of Natural History Sciences, Hokkaido University, Sapporo 060-0810, JAPAN

[2] Department of Cosmosciences, Hokkaido University, Sapporo 060-0810, JAPAN

[3] Hawai'i Institute of Geophysics and Planetology, School of Ocean and Earth Science and Technology, University of Hawai'i at Manoa, Honolulu, HI 96822, USA

[4] Isotope Imaging Laboratory, Creative Research Initiative "Sousei", Hokkaido University, Sapporo, 001-0021, Japan

*To whom correspondence should be addressed. E-mail: yuri@ep.sci.hokudai.ac.jp

Abstracts

Oxygen isotopic composition of our Solar System is believed to have resulted from mixing of two isotopically distinct nebular reservoirs, ^{16}O-rich and ^{17,18}O-rich relative to the Earth. The nature and composition of the ^{17,18}O-rich reservoir are poorly constrained. We report an in situ discovery of a chemically and isotopically unique material distributed ubiquitously in fine-grained matrix of a primitive carbonaceous chondrite Acfer 094. This material formed by oxidation of Fe,Ni-metal and sulfides by water either in the solar nebula or on a planetecimal. Oxygen isotopic composition of this material indicates that the water was highly enriched in ^{17}O and ^{18}O ($\delta^{17,18}O_{SMOW}$ =+180‰), providing the first evidence for an extremely ^{17,18}O-rich reservoir in the early Solar System.

Text

Oxygen isotopic variations in chondrites provide important constraints on the origin and early evolution of the Solar System (*1*). Oxygen isotope ratios in chondrites change not only by mass-dependent isotope fractionation law (isotope fractionation depending on mass differences among isotopes), but also by large mass-independent isotope fractionation (MIF) that keeps ^{17}O/^{18}O ratio nearly constant. It is generally accepted that MIF recorded by meteorites resulted from mixing of two isotopically distinct nebular reservoirs, ^{16}O-rich and ^{17,18}O-rich (*2*). The composition of the ^{16}O-rich reservoir has been recently constrained from isotopic compositions of nebular condensates (*3*) and of a unique

chondrule (*4*). The nature and composition of an ^{17,18}O-rich nebular reservoir are still poorly constrained (*5, 6*). According to the currently favorite self-shielding models (*7-11*), nebular water is hypothesized to have been highly enriched in ^{17,18}O (5-20%) relative to the Earth, which is, however, yet to be verified by isotope measurements. Here we report an in situ discovery of a chemically and isotopically unique material in the primitive carbonaceous chondrite Acfer 094. This material is mainly composed of iron, oxygen, and sulfur, and is highly enriched in ^{17}O and ^{18}O (up to +18%) relative to the Earth's ocean. Mineralogical observations and thermodynamic analysis suggest that this material resulted from oxidation of iron-metal and/or iron-sulfide by water in the solar nebula or on a planetesimal. We infer that the extreme oxygen isotopic composition of this material recorded composition of this primordial water, that corresponds to an ^{17,18}O-rich nebular reservoir in the early Solar System, in agreement with the self-shielding models (*7-12*).

During our on-going in situ survey (*13-16*) of presolar grains of primitive meteorites (*17*), we discovered isotopically anomalous regions of oxygen in matrix of the ungrouped carbonaceous chondrite Acfer 094 in addition to isotopically anomalous spots corresponding to presolar grains (Fig. 1). The oxygen isotopic compositions of the regions are uniform and enriched in ^{17}O and ^{18}O relative to ^{16}O (Fig. 2). The data seem to be plotted along the slope-1 line (*18*) rather than the carbonaceous chondrite anhydrous mineral mixing (CCAM) line (*2*) (Fig. 3). The representative values of $\delta^{17}O_{SMOW} = \delta^{18}O_{SMOW}$ are

about +180‰[1]. These are the heaviest oxygen isotopic compositions of the Solar System materials reported so far. The less ^{17}O- and ^{18}O-rich compositions ($\delta^{17,18}O_{SMOW}$ =+50‰) of unknown origin have been recently reported in the surface layers of metal grains from lunar regolith (*19*).

The chemical compositions of the isotopically anomalous regions determined by an energy dispersive X-ray spectrometer (EDS) attached to a field-emission type scanning electron microscope (FE-SEM) *(16)* show that they are homogeneous and mainly composed of Fe, Ni, O and S (representatively, in wt%, Fe, 61.6; Ni, 5.4; O, 19.3; S, 9.6; Mg, 0.1; Si, 0.2). In addition, analytical transmission electron microscopy (ATEM) *(16)* reveals that the regions consist of aggregates of nanocrystals with a size range of 10-200 nm (Fig. S1). The electron diffraction patterns from ~100-nm-sized individual crystals show that the main spots of the crystals are similar to those of magnetite (Fe_3O_4; space group *Fd3m*); the corresponding cell parameter *a* is 0.83 nm. In addition, there are weak extra spots suggesting a 3-fold superstructure. Characteristic X-ray spectra from individual crystals show that they consist of the same elements determined by the FE-SEM-EDS study. These observations indicate that the crystals have a magnetite-like structure and may represent a new Fe-O-S-bearing mineral; more detail characterization is necessary to identify it. Although this mineral consists of the same elements as a poorly characterized phase (PCP)

[1] $\delta^{i}O_{SMOW}$ (‰) $\equiv[(^{i}O/^{16}O)_{sample}/(^{i}O/^{16}O)_{SMOW} -1]\times1000$ where i =17 or 18 and SMOW is the standard mean ocean water.

commonly observed in aqueously altered CM chondrites and largely composed of tochilinite or tochilinite-cronstedtite intergrowths (*20, 21*), its O/S atom ratios are about 4 times larger than in tochilinite. Hereafter we refer to this mineral as a new-PCP.

The chemically unique and isotopically anomalous new-PCPs are ubiquitous and scattered randomly throughout the Acfer 094 matrix. Twenty-two new-PCPs (the largest is 160 μm^2) were identified in about 11mm^2 area of the matrix using elemental mapping with a 7 μm^2 spatial resolution. This corresponds to 94±20 (σ) parts per million (ppm) by volume. Because the number of the new-PCP grains increases exponentially with decreasing size, the grain numbers below 7 μm^2 are dominant and the actual abundance of new-PCP must be larger than the estimate.

The new-PCP often coexists with troilite (FeS) (Fig. 2) which is considered to be a reaction product between Fe, Ni-metal and H_2S gas (*22, 23*).

$$Fe + H_2S = FeS + H_2 \qquad (1)$$

Because new-PCP has the magnetite-like diffraction patterns, magnetite can be used as its proxy. Magnetite can be formed by oxidation of Fe, Ni-metal (*22, 24*) or troilite.

$$3Fe + 4H_2O = Fe_3O_4 + 4H_2 \qquad (2)$$

$$3FeS + 4H_2O = Fe_3O_4 + 3H_2S + H_2 \qquad (3)$$

Oxidation of troilite or metal to form new-PCP would occur below 360K independent on total pressure of the solar nebula (Fig. 4). If the nebular P_{H2O}/P_{H2} ratio increases from a characteristic value for a gas of solar composition (*24*), formation of

new-PCP occurs at higher temperature. Although, the complete chemical equilibrium would not be expected in the cool solar nebula (*22*), the new-PCP would be formed inside the water sublimation front (snowline) of the solar nebula because water vapor is the major oxidant in the solar nebula and the sublimation temperature of water ice is below 200K even in the several-fold H_2O-enriched nebula (*22*).

Alternatively, new-PCP may have been formed by aqueous alteration of metal and troilite on the Acfer 094 parent body, like tochilinite in the aqueously altered CM chondrites (*21*). In order to test this hypothesis, we analyzed oxygen isotopic compositions of tochilinite in the CM chondrite Murchison. In contrast to the Acfer 094 new-PCP, oxygen isotopic composition of the Murchison tochilinite is plotted near the terrestrial fractionation line, along the "CM waters" line (*26*) (Fig. 3), that is considered to be a reaction path between aqueous solution and matrix silicates toward the isotope equilibrium (*26*). These observations and the lack of mineralogical and petrographical evidence of aqueous alteration of Acfer 094 (*27*) exclude formation of new-PCP by the aqueous alteration previously observed in chondrites. If new-PCP resulted from oxidation of troilite or metal in a planetesimal setting, a plausible oxidant would be water vapor or aqueous solution which originated from accreted nebular ice and did not experience oxygen isotope exchange with the matrix silicates. In contrast, the inferred oxygen isotopic compositions (*26, 28*) and the observational most ^{17,18}O-rich composition (*29*) of chondrite-parent body water may have recorded equilibration of aqueous solutions with the chondrite matrix

silicates.

We conclude that oxygen isotopic compositions of new-PCP in Acfer 094 represent composition of the primordial water of the Solar System and the previously hypothesized ^{17}O- and ^{18}O-rich reservoir in the early Solar System. The wide oxygen isotopic variations of at least -80‰ $<\delta^{17,18}O<$ +180‰ found from hot and cold origin materials must provide new guidelines for the origin of oxygen isotope anomaly in the solar system.

References and notes

1. R. N. Clayton, *Science* **313**, 1743 (2006).
2. R. N. Clayton, *Annu. Rev. Earth Planet. Sci.* **21**, 115 (1993).
3. A. N. Krot, K. D. McKeegan, L. A. Leshin, G. J. MacPherson, E. R. D. Scott, *Science* **295**, 1051 (2002).
4. S. Kobayashi, H. Imai, H. Yurimoto, *Geochem. J.* **37**, 663 (2003).
5. H. Yurimoto, M. Ito, H. Nagasawa, *Science* **282**, 1874 (1998).
6. A. N. Krot *et al.*, *Astrophys. J.* **622**, 1333 (2005).
7. R. N. Clayton, *Nature* **415**, 860 (2002).
8. H. Yurimoto, K. Kuramoto, *Meteorit. Planet. Sci.* **37**, A153 (2002).
9. H. Yurimoto, K. Kuramoto, *Science* **305**, 1763 (2004).
10. J. R. Lyons, E. D. Young, *Nature* **435**, 317 (2005).

11. H. Yurimoto *et al*., in *Protostars and Planets V* B. Reipurth, D. Jewitt, K. Keil, Eds. (University of Arizona Press, Tucson, 2007) pp. 849–862.

12. E. D. Young, *Lunar Planet. Sci.* **XXXVII**, Abstract #1790 (2006).

13. H. Yurimoto, K. Nagashima, T. Kunihiro, *Appl. Surf. Sci*. **203-204**, 793 (2003).

14. S. Itoh, H. Yurimoto, *Nature* **423**, 728 (2003).

15. T. Kunihiro, K. Nagashima, H. Yurimoto, *Geochim. Cosmochim. Acta* **69**, 763 (2005).

16. Materials and methods are available as supporting material on Science Online.

17. K. Nagashima, A. N. Krot, H. Yurimoto, *Nature* **428**, 921 (2004).

18. E. D. Young, S. S. Russell, *Science* **282**, 452 (1998).

19. T. R. Ireland, P. Holden, M. D. Norman, J. Clarke, *Nature* **440**, 776 (2006).

20. L. H. Fuchs, E. Olsen, K. J. Jensen, *Smison. Contrib. Earth Sci.* **10**, 1 (1973).

21. K. Tomeoka, P. R. Buseck, *Geochim. Cosmochim. Acta* **49**, 2149 (1985).

22. B. Fegley, Jr., *Space Sci. Rev.* **92**, 177 (2000).

23. D. S. Lauretta, D. T. Kremser, B. Fegley, Jr., *Icarus* **122**, 288 (1996).

24. Y. Hong, B. Fegley, Jr., *Meteorit. Planet. Sci.* **33**, 1101 (1997).

25. A. N. Krot, B. Fegley, Jr., K. Lodders, H. Palme, in *Protostars and Planets IV* V. Mannings, A. P. Boss, S. S. Russell, Eds. (The University Arizona Press, Tucson, 2000) pp. 1019-1054.

26. R. N. Clayton, T. K. Mayeda, *Geochim. Cosmochim. Acta* **63**, 2089 (1999).

27. A. Greshake, *Geochim. Cosmochim. Acta* **61**, 437 (1997).

28. E. D. Young, *Phil. Tran. R. Soc. Lond. A* **359**, 2095 (2001).

29. B.-G. Choi, K. D. McKeegan, A. N. Krot, J. T. Wasson, *Nature* **392**, 577 (1998).

30. J. M.W. Chase, *NIST-JANAF Thermochemical Tables, Fourth edition, Journal of Physical and Chemical Reference Data, Monograph 9, (Part I and Part II)* (American Institute of Physics, New York, 1998), pp. 1963.

31. We thank Y. Matsuhisa for providing a magnetite standard, T. Kaito and I. Nakatani for assistance of FIB sample preparation, K. Tomeoka for indicating Murchison tochilinite, and E. D. Scott and G. R. Huss for discussion. This work was partly supported by Monkasho (H.Y.) and NASA (A.N.K.).

Figure legends

Fig. 1. Spatial distribution of $^{17}O/^{16}O$ in matrix of the ungrouped carbonaceous chondrite Acfer 094 measured using isotopography *(16)*. An isotopically anomalous 10 μm-sized region ($\delta^{17}O_{SMOW}$=+180‰) and a spot ($\delta^{17}O_{SMOW}$=+400‰) are surrounded by the isotopically normal matrix materials. The spot corresponds to a presolar silicate grain, whereas the isotopically anomalous region corresponds to a new-PCP.

Fig. 2. Oxygen isotopic distribution and grain shape for new-PCP embedded in chondrite matrix. $\delta^{17}O_{SMOW}$ (A, D), $\delta^{18}O_{SMOW}$ (B, E) and backscattered electron (C, F) images

for new-PCP #14 (A-C) and #21 (D-F) in the Acfer 094 matrix. Arrow in (A) indicates small troilite grains attached to the new-PCP #14. The new-PCP #21 is surrounded by troilite. Because troilite contains no oxygen, the troilite area in (D) and (E) is masked by black color. The new-PCPs are highly enriched in ^{17}O and ^{18}O isotopes relative to the matrix.

Fig. 3. Oxygen isotopic compositions of the new-PCP from the Acfer 094 matrix. Oxygen isotopic compositions of matrix and amoeboid olivine aggregate (AOA) from Acfer 094 and tochilinite from Murchison are also plotted. The new-PCPs are plotted on extrapolation of slope-1 line or carbonaceous chondrite anhydrous mineral mixing (CCAM) line. The compositions of the Murchison tochilinite are plotted near the terrestrial fractionation (TF) line, along an aqueous alternation line (CM waters (*26*)). Isotopography: analyzed by precise isotopic imaging using isotope microscope *(16)*. Point SIMS: analyzed by conventional point analysis by SIMS *(16)*, The data are listed in Table S1.

Fig. 4. Calculated equilibrium temperatures for Fe-metal, troilite (FeS) and magnetite (Fe_3O_4) as a function of P_{H2S}/P_{H2} ratio. The magnetite phase boundary is calculated assuming canonical solar nebular H_2O/H_2 ratio of 5×10^{-4} (*25*). Magnetite is considered as a proxy of a new-PCP. Thermodynamic data from NISI-JANAF tables (*30*) were used for calculations.

Fig. 1.

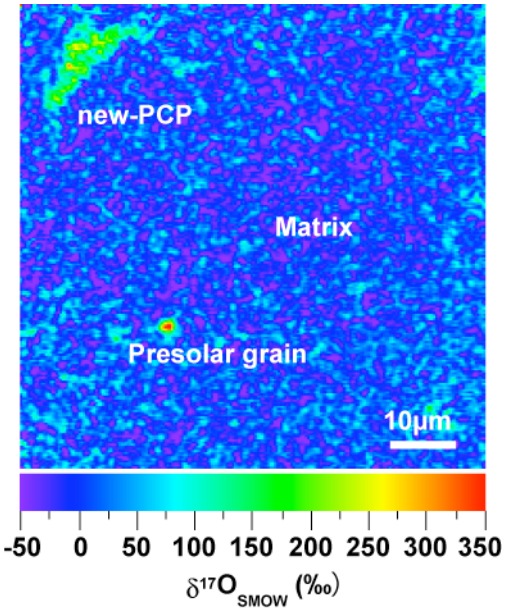
new-PCP
Matrix
Presolar grain
10μm
-50 0 50 100 150 200 250 300 350
δ17OSMOW (‰)

Fig. 2.

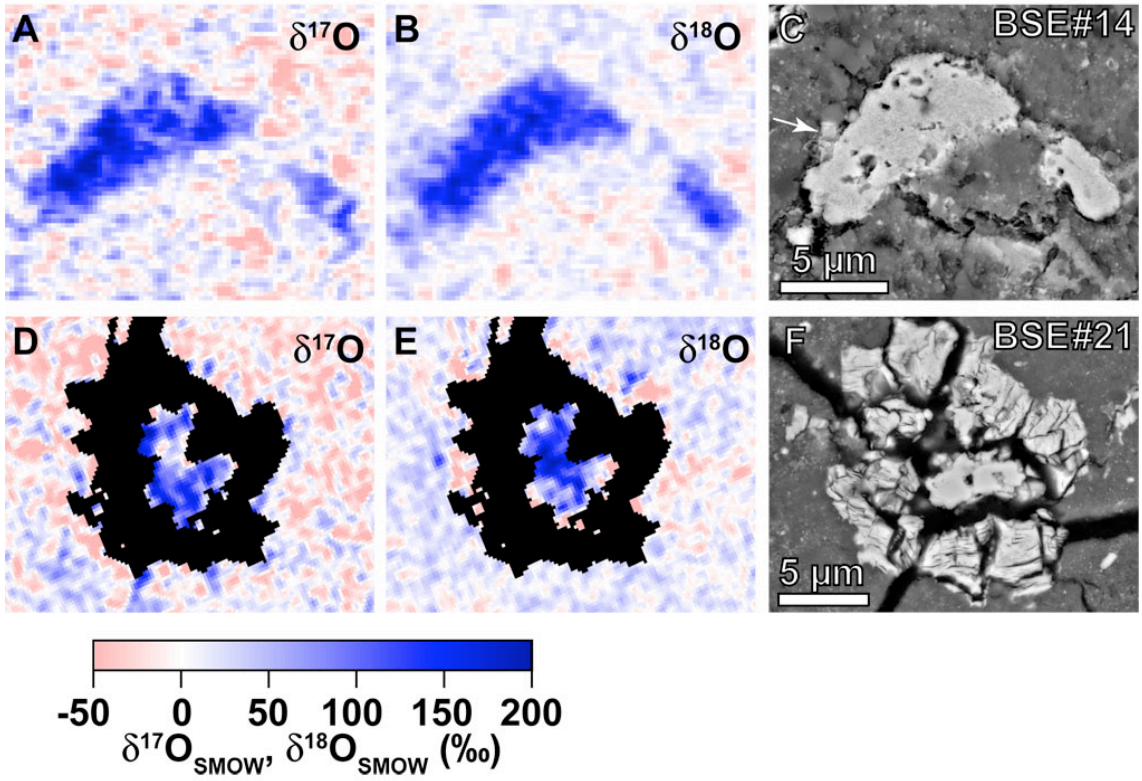
A
δ17O
B
δ18O
C
BSE#14
5 μm
D
δ17O
E
δ18O
F
BSE#21
5 μm
-50
0
50
100
150
200
δ17OSMOW, δ18OSMOW (‰)

Fig. 3.

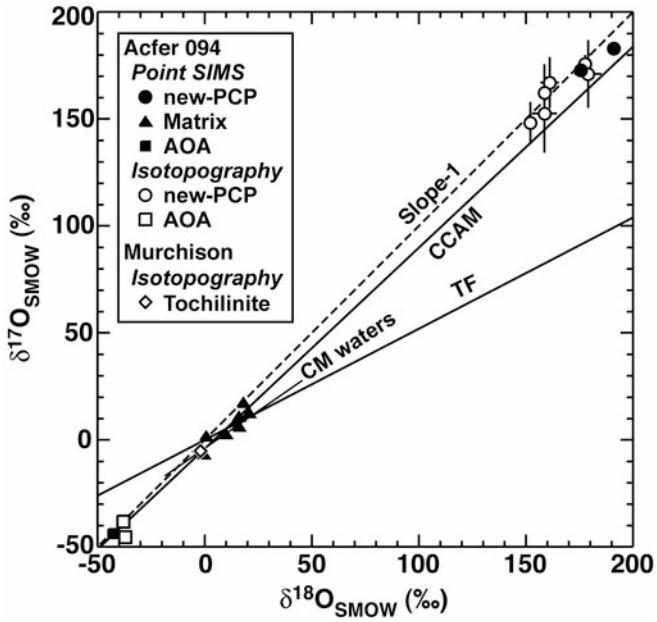
Acfer 094
Point SIMS
new-PCP
Matrix
AOA
Isotopography
new-PCP
AOA
Murchison
Isotopography
Tochilinite
Slope-1
CCAM
CM waters
TF
δ17OSMOW (‰)
δ18OSMOW (‰)
200
150
100
50
0
-50
-50
0
50
100
150
200

Fig. 4.

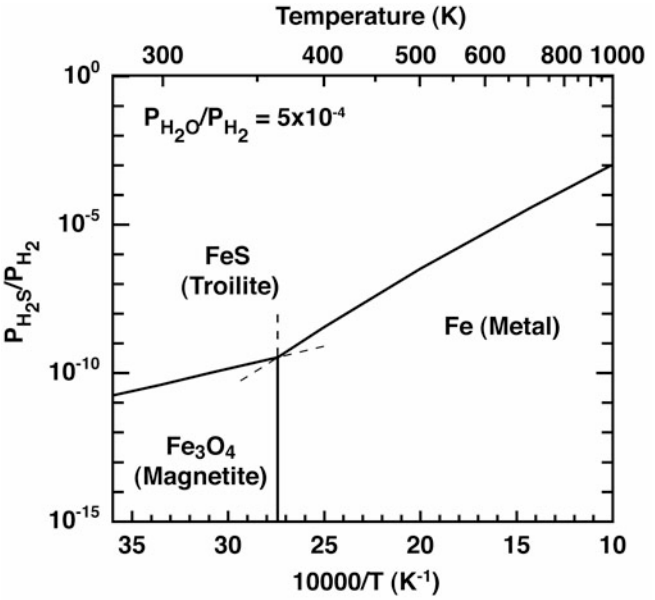
Temperature (K)
300
400
500
600
800
1000
10^0
10^{-5}
10^{-10}
10^{-15}
P_{H_2O}/P_{H_2} = 5x10^{-4}
FeS
(Troilite)
Fe (Metal)
Fe_3O_4
(Magnetite)
P_{H_2S}/P_{H_2}
35
30
25
20
15
10
10000/T (K^{-1})

Supporting Online Material

Materials and Methods

A polished thin section of a primitive carbonaceous chondrite Acfer 094 has been prepared for this study. The thin section was coated by a carbon evaporation film of about 30 nm in order to reduce electrostatic charging during high-energy electron and ion bombardments for chemical and isotopic analyses. A field-emission type scanning electron microscope (FE-SEM, JEOL JSM-7000F) equipped with an energy dispersive X-ray spectrometer (EDS, Oxford INCAEnergy) has been used to analyze petrographical texture and chemical compositions.

A Hokudai isotope microscope system *(S1)* (Cameca ims-1270 + SCAPS; originally installed in Tokyo Institute of Technology and now in Hokkaido Univ. (Hokudai)) has been used to image precise isotope distribution (isotopography) *(S2)* in the chondrite matrices. A Cs^+ primary beam of 20 keV was homogeneously irradiated on the sample surface of approximately 80 μm in diameter with a beam current of ~0.3 nA. A normal incident electron gun was used to compensate positive charging of the sputtered region due to the primary beam. We obtained secondary ion images of $^{12}C^-$, $^{13}C^-$, $^{12}C^-$, $^{27}Al^-$, $^{28}Si^-$, $^{16}O^-$, $^{18}O^-$, $^{16}O^-$, $^{17}O^-$, and $^{16}O^-$ sequentially for one analytical sequence. The exposure time was 20 seconds for $^{12}C^-$, 1000 seconds for $^{13}C^-$, 100 seconds for $^{27}Al^-$, 200 seconds for $^{28}Si^-$, 20 seconds for $^{16}O^-$, 3200 seconds for $^{17}O^-$ and 1600 seconds for $^{18}O^-$ isotopography. A 50 μm contrast aperture was used and the secondary ion contributions except for

objective isotopes were cut by the exit slit. Beam irradiation time for the sequence was ~2 hour. The sputtering depth was less than 200 nm for the sequence. Typical spatial resolution under the condition of isotopography was ~0.3 μm. The width of a pixel of SCAPS corresponds to 0.2 μm on the sample surface. An image processing method of moving average with 3 × 3 pixels was applied to Figures 1 and 2 to reduce the statistical error due to small ion integration of ^{17}O and ^{18}O. As a result, a spatial resolution of Figures 1 and 2 is 0.6 μm, and the oxygen isotopic precision per the spatial resolution is ±25‰ (σ) for $\delta^{17}O_{SMOW}$ and ±10‰ (σ) for $\delta^{18}O_{SMOW}$. On the other hand, the standard deviations of Table S1 were calculated from original image without the image processing. Other analytical methods for isotopography were described in detail elsewhere *(S1, S2)*.

A conventional point analysis of secondary ion mass spectrometry (SIMS) has been also applied to determine oxygen isotopic compositions using the Cameca ims-1270. An oval-shaped Cs^+ ion micro-probe (2.0 × 1.3 μm^2) with 20 keV was used. Secondary ions of $^{16}O^-$-tail, $^{16}O^-$, $^{17}O^-$, $^{16}OH^-$, and $^{18}O^-$ were measured by an electron multiplier. Terrestrial magnetite and olivine standards were used to normalize secondary ion-ratios to the $\delta^{17,18}O_{SMOW}$-values for new-PCP and silicates, respectively. Other analytical procedures were described in detail elsewhere *(S3)*.

Dead time correction of the electron multiplier would introduce an analytical artifact of systematic shift of oxygen isotopic compositions along the slope-1 line of Fig. 3. The dead time is estimated to be 16.0±0.5 ns by measurements of Ti isotopes. Because the

dead time correction mainly modifies secondary ion intensities of the most dominant oxygen isotope, the count rates and the counting losses estimated by the dead time are shown in Table S2 for each measurement point. All measurements have been carried out similar conditions of secondary ion emission. Estimated counting losses of secondary ion intensities are smaller than oxygen isotopic variations between new-PCP and other phases. Such dead time corrections are not necessary to consider for the isotopography because the SCAPS is an integral type detector.

An analytical transmission electron microscope (ATEM, JEOL JEM-2010) equipped with EDS (Thermo Electron Noran system SIX) has been used to analyze crystal structure, crystal size, texture and compositions. A sample for ATEM study was directly cut out from the thin section by focused ion beam (FIB) method using SII NanoTechnology SMI3050TB instrument. A film of ~8μm × 8μm × 50 nm was prepared and a 200 keV electron beam was used for the observation.

References

1. H. Yurimoto, K. Nagashima, T. Kunihiro, *Applied Surface Science* **203-204**, 793 (2003).

2. T. Kunihiro, K. Nagashima, H. Yurimoto, *Geochim. Cosmochim. Acta* **69**, 763 (2005).

3. S. Itoh, H. Yurimoto, *Nature* **423**, 728 (2003).

Fig. S1 (A) Transmission electron micrograph showing the texture of new-PCP. (B) a diffraction pattern and (C) an X-ray elemental spectrum from a single new-PCP grain. The main spots in the diffraction pattern are similar to those of magnetite (space group *Fd3m*); the weak extra spots indicate a 3-fold superstructure. This pattern is viewed along [111] of the *Fd3m* cell of the main spots.

Table S1

Table S1. Oxygen isotopic compositions (‰) of new-PCPs, tochilinite, matrix and AOA of meteorites. Averaging areas: # of analysis areas (μm^2) used for averaging. $\Delta^{17}O_{SMOW} = \delta^{17}O_{SMOW} - 0.52\delta^{18}O_{SMOW}$.

Object name	Analysis area	Averaging areas	$\delta^{17}O_{SMOW}$	σ_{mean}	$\delta^{18}O_{SMOW}$	σ_{mean}	$\Delta^{17}O$
Isotopography							
new-PCP of Acfer 094							
#14	0.8 x 0.8	5	167	12	161	4	83
#15	0.8 x 0.8	5	162	13	159	2	80
#17	2.0 x 2.0	5	176	4	178	3	83
#19	0.6 x 0.4	5	148	10	152	1	69
#20	0.6 x 0.6	5	153	18	159	6	70
#21	0.4 x 0.6	3	171	9	179	4	78
Tochilinite of Murchison							
#38	2.0 x 2.0	5	-5	2	-2	3	-4
AOA of Acfer 094							
#18	3.2 x 3.2	5	-45	4	-37	2	-26
#23	4.0 x 4.0	5	-38	2	-38	1	-18
Point SIMS							
new-PCP of Acfer 094							
#17-s29	2.0 x 1.3	1	183	3	191	2	84
#17-s47	2.0 x 1.3	1	173	4	176	3	82
Matrix of Acfer 094							
#s39	2.0 x 1.3	1	2	2	1	2	1
#s40	2.0 x 1.3	1	3	2	10	2	-2
#s41	2.0 x 1.3	1	18	3	18	2	8
#s43	2.0 x 1.3	1	9	2	15	1	1
#s44	2.0 x 1.3	1	13	3	21	2	2
#s45	2.0 x 1.3	1	-7	3	0	2	-6
#s46	2.0 x 1.3	1	11	2	16	2	3
#s49	2.0 x 1.3	1	6	2	16	2	-2
mean		8	7	3	12	3	1
AOA of Acfer 094							
#s50	2.0 x 1.3	1	-44	3	-43	2	-21

Isotopography: extracted from an isotope image by SCAPS using imaging SIMS. Point SIMS: measured by an electron multiplier using an oval-shaped ion micro-probe. AOA: ameoboid olivine aggregate.

Table S2

Table S2. Secondary ion count rate (cps) and calculated counting loss (%) of $^{16}O^-$ secondary ion for each measurement piont.

Object name	Count rate	Counting loss
new-PCP of Acfer 094		
#17-s29	5.3E+05	0.9
#17-s47	3.4E+05	0.5
Matrix of Acfer 094		
#s39	4.1E+05	0.6
#s40	3.6E+05	0.6
#s41	3.6E+05	0.6
#s43	4.0E+05	0.6
#s44	3.6E+05	0.6
#s45	3.2E+05	0.5
#s46	4.1E+05	0.7
#s49	4.4E+05	0.7
AOA of Acfer 094		
#s50	3.8E+05	0.6
Standard		
Olivine	4.1E+05	0.6
Magnetite	4.5E+05	0.7

Fig. S1.